

Thermal-contact capacity of one-dimensional attractive Gaudin-Yang model

Xiao-Min Zhang(张小敏), Song Cheng(程颂), and Yang-Yang Chen(陈洋洋)

Citation: Chin. Phys. B, 2024, 33 (**4**): 040203. DOI: 10.1088/1674-1056/ad21f4
Journal homepage: http://cpb.iphy.ac.cn; http://iopscience.iop.org/cpb

What follows is a list of articles you may be interested in

Quintessence anisotropic stellar models in quadratic and Born-Infeld modified teleparallel Rastall gravity

Allah Ditta, Tiecheng Xia(夏铁成), Irfan Mahmood, and Asif Mahmood
Chin. Phys. B, 2024, 33 (**3**): 030204. DOI: 10.1088/1674-1056/acfaf9

Exact solutions for magnetohydrodynamic nanofluids flow and heat transfer over a permeable axisymmetric radially stretching/shrinking sheet

U. S. Mahabaleshwar, G. P. Vanitha, L. M. Pérez, Emad H. Aly, and I. Pop
Chin. Phys. B, 2024, 33 (**2**): 020204. DOI: 10.1088/1674-1056/ad09c9

MetaPINNs: Predicting soliton and rogue wave of nonlinear PDEs via the improved physics-informed neural networks based on meta-learned optimization

Yanan Guo(郭亚楠), Xiaoqun Cao(曹小群), Junqiang Song(宋君强), and Hongze Leng(冷洪泽)
Chin. Phys. B, 2024, 33 (**2**): 020203. DOI: 10.1088/1674-1056/ad0bf4

Soliton propagation for a coupled Schrödinger equation describing Rossby waves

Li-Yang Xu(徐丽阳), Xiao-Jun Yin(尹晓军), Na Cao(曹娜) and Shu-Ting Bai(白淑婷)
Chin. Phys. B, 2023, 32 (**7**): 070202. DOI: 10.1088/1674-1056/acb9e5

Exact solution of the Gaudin model with Dzyaloshinsky-Moriya and Kaplan-Shekhtman-Entin-Wohlman-Aharony interactions

Fa-Kai Wen(温发楷) and Xin Zhang(张鑫)
Chin. Phys. B, 2021, 30 (**5**): 050201. DOI: 10.1088/1674-1056/abcf43

Thermal-contact capacity of one-dimensional attractive Gaudin–Yang model

Xiao-Min Zhang(张小敏)[1], Song Cheng(程颂)[2,†], and Yang-Yang Chen(陈洋洋)[1,3,4,‡]

[1] *Institute of Modern Physics, Northwest University, Xi'an* 710069, *China*
[2] *Beijing Computational Science Research Center, Beijing* 100193, *China*
[3] *Peng Huanwu Center for Fundamental Theory, Northwest University, Xi'an* 710069, *China*
[4] *Shaanxi Key Laboratory for Theoretical Physics Frontiers, Northwest University, Xi'an* 710069, *China*

(Received 31 October 2023; revised manuscript received 25 December 2023; accepted manuscript online 24 January 2024)

Tan's contact $\mathcal{C}$ is an important quantity measuring the two-body correlations at short distances in a dilute system. Here we make use of the technique of exactly solved models to study the thermal-contact capacity $\mathcal{K}_{\rm T}$, i.e., the derivative of $\mathcal{C}$ with respect to temperature in the attractive Gaudin–Yang model. It is found that $\mathcal{K}_{\rm T}$ is useful in identifying the low temperature phase diagram, and using the obtained analytical expression of $\mathcal{K}_{\rm T}$, we study its critical behavior and the scaling law. Especially, we show $\mathcal{K}_{\rm T}$ versus temperature and thus the non-monotonic tendency of $\mathcal{C}$ in a tiny interval, for both spin-balanced and imbalanced phases. Such a phenomenon is merely observed in multi-component systems such as $SU(2)$ Fermi gases and spinor bosons, indicating the crossover from the Tomonaga–Luttinger liquid to the spin-coherent liquid.

Keywords: Tan's Contact, Gaudin–Yang model, Bethe ansatz

PACS: 02.30.Jr, 07.07.Df, 07.05.Dz **DOI:** 10.1088/1674-1056/ad21f4

1. Introduction

It is remarkable that the concept of Tan's contact $\mathcal{C}$ captures the universal properties of dilute systems, building up relations among the tail of momentum distribution, pair correlation function and energy, etc.[1–4] Although the definition of contact does not rely on any specified matter phase, its behavior near the quantum critical point has gained much interest and much progress has been made.[5–7] In a generalized Maxwell relation, the contact is considered as the partial derivative of thermodynamic potential over interaction strength,[5] which gives a possibility to study the dependence of contact on various other driving parameters of systems. One can define this type of relation as contact capacity, such as the magnetic-contact capacity $\mathcal{K}_m = \partial\mathcal{C}/\partial H$ describing how much contact is contained in a magnetic field unit.[6] The critical behavior of $\mathcal{K}_m$ was firstly studied in the Gaudin–Yang model by utilizing the Bethe ansatz technique.[6]

The two-component Fermi gas of contact interaction in one dimension is a quantum integrable model named after Gaudin and Yang, in honor of their contribution to its first analytical resolution.[8,9] As a paradigm model of condensed matter physics, it serves as a versatile platform for investigating a variety of novel physics for instance, the dimensionless quantities Wilson ratio[10] and Grüneisen parameter,[7] quantum phase transitions,[11] Fulde–Ferrell–Larkin–Ovchinnikov (FFLO) phase[12,13] and BCS–BEC crossover, etc. See a review[14] for more details.

In this article, we study the thermal-contact capacity of the attractive Gaudin–Yang model by employing the Bethe ansatz technique numerically and analytically. We show that this quantity is helpful in determining the low temperature phase diagram, and in both spin-balanced and spin-imbalanced phases the dramatic changes of $\mathcal{K}_{\rm T}$ in low temperatures indicates a non-monotonic behavior of $\mathcal{C}$, and thus the crossover of the system from the Tomonaga–Luttinger liquid phase to the spin-incoherent phase. Moreover, we study the scaling law of $\mathcal{K}_{\rm T}$ by virtue of the analytical expression obtained in strong coupling regime, read off the critical exponents and scaling function, and map out the phase boundary.

2. Model and methods

The Hamiltonian of the Gaudin–Yang model reads[15]

$$\mathcal{H} = -\frac{\hbar^2}{2m}\sum_{i=1}^{N}\frac{\partial^2}{\partial x_i^2} + 2c\sum_{1\le i<j\le N}\delta(x_i - x_j) - \mu N - \frac{1}{2}H(N-2M), \tag{1}$$

where N is the total particle number, M the down-spin particle number, μ the chemical potential, H the magnetic field, and $c<0$ ($c>0$) specifies the strength of attraction (repulsion) between two particles. In the following, we only study the attractive situation, and for the sake of simplicity let $\hbar = 2m = 1$. Taking periodic boundary condition, the diagonalization of the above Hamiltonian is transformed into solving the following

†Corresponding author. E-mail: scheng@csrc.ac.cn
‡Corresponding author. E-mail: chenyy@nwu.edu.cn

© 2024 Chinese Physical Society and IOP Publishing Ltd

Bethe ansatz equations (BAE):

$$e^{ik_jL}=\prod_{\alpha=1}^{M}\frac{k_j-\Lambda_\alpha+ic/2}{k_j-\Lambda_\alpha-ic/2},\quad j=1,\ldots,N,$$
$$\prod_{j=1}^{N}\frac{\Lambda_\alpha-k_j+ic/2}{\Lambda_\alpha-k_j-ic/2}=-\prod_{\beta=1}^{M}\frac{\Lambda_\alpha-\Lambda_\beta+ic}{\Lambda_\alpha-\Lambda_\beta-ic},\ \alpha=1,\ldots,M,\quad(2)$$

where k_j and Λ_α are the j-th quasimomentum and the α-th spin rapidity, respectively. As the solution to BAE, both $\{k\}$ and $\{\Lambda\}$ can be complex numbers. In thermodynamic limit, their distribution on complex plane obeys the string hypothesis.[15] Both $\{k\}$ and $\{\Lambda\}$ can be either purely real or complex, the $2M'$ complex-valued k and the M' real-valued Λ may form the $k-\Lambda$ strings, namely,

$$k_\alpha^1=\Lambda_\alpha'+\frac{i}{2}c,\ \ k_\alpha^2=\Lambda_\alpha'-\frac{i}{2}c,\ \ \alpha=1,2,\ldots,M';\quad(3)$$

the other Λ, being complex-valued, may form the Λ–Λ strings of different lengths as follows:

$$\Lambda_{\alpha,j}^n=\Lambda_\alpha^n+\frac{i}{2}(n+1-2j)c,\ \ j=1,2,\ldots,n,$$
$$\alpha=1,2,\ldots,M_n,\quad(4)$$

where the real-valued Λ_α^n is the center of the α-th length-n string, and $M'+\sum_n nM_n=M$. Utilizing the string hypothesis in combination with the standard Yang–Yang approach yields the thermodynamic Bethe ansatz (TBA) equations.[15] At finite temperature, they usually consist of infinitely many coupled integral equations. Specifically to the attractive Gaudin–Yang model, they can be expressed as

$$\begin{aligned}\varepsilon_u(k)=&k^2-\mu-\frac{H}{2}+Ta_1*\ln[1+e^{-\varepsilon_b(k)/T}]\\&-T\sum_{m=1}^{\infty}a_m*\ln[1+\eta_m^{-1}(k)],\\\varepsilon_b(k)=&2\left(k^2-\mu-\frac{c^2}{4}\right)+Ta_2*\ln[1+e^{-\varepsilon_b(k)/T}]\\&+Ta_1*\ln[1+e^{-\varepsilon_u(k)/T}],\\\ln\eta_n(\lambda)=&\frac{nH}{T}+a_n*\ln[1+e^{-\varepsilon_u(\lambda)/T}]\\&+\sum_{m=1}^{\infty}T_{nm}*\ln[1+\eta_m^{-1}(\lambda)],\end{aligned}\quad(5)$$

where $a_n(x)=\frac{1}{2\pi}\frac{n|c|}{(nc/2)^2+x^2}$, the convolution operator $*$ means $a*f(x)=\int_{-\infty}^{\infty}a(x-y)f(y)dy$, see Appendix A for $T_{nm}(x)$. Here $\eta_n(\lambda)$ is a function describing the distribution of the real-valued centers for those complex-valued spin rapidities on length-n strings.[16] The dressed energy $\varepsilon_u(k)$ ($\varepsilon_b(k)$) can be considered as the elementary excitation of adding a single particle (bound pair) of quasimomentum k to the ground state, which are very useful in formulating the pressure

$$p=\frac{T}{\pi}\int\ln\left(1+e^{-\frac{\varepsilon_b(k)}{T}}\right)dk+\frac{T}{2\pi}\int\ln\left(1+e^{-\frac{\varepsilon_u(k)}{T}}\right)dk.\quad(6)$$

It is interesting to point out that the pressure of the system is the addition of two parts, one from the polarized particles and the other from the bound pairs.

In principle, all the thermodynamic quantities can be expressed in terms of dressed energies by taking first or second derivatives of pressure over relevant driving variables, such as the magnetization $m=\partial p/\partial H$ and the compressibility $\kappa_c=\partial^2 p/\partial\mu^2$. Similarly, Tan's contact is readily obtained by taking derivative of pressure over the contact interaction

$$\mathcal{C}=-\frac{c^2}{2}\frac{\partial p}{\partial c},\quad(7)$$

and its dependence on temperature follows

$$\frac{\partial\mathcal{C}}{\partial T}=-\frac{c^2}{2}\frac{\partial^2 p}{\partial c\partial T}=-\frac{c^2}{2}\frac{\partial S}{\partial c},\quad(8)$$

where S is the entropy on unit length. Noting the presence of binding energy $\varepsilon_B=c^2/2$, we define the thermal-contact capacity, a dimensionless quantity, as

$$\mathcal{K}_T\equiv\frac{1}{\varepsilon_B}\frac{\partial\mathcal{C}}{\partial T}=-\frac{\partial S}{\partial c},\quad(9)$$

to measure the volume of contact around a specified temperature for a Gibbs ensemble, which is related to the Grüneisen parameter as well.[7]

3. Results

The quantum phase transitions of the model are continuous. In accordance with this and Eq. (7), Tan's contact does not show significant change in the critical region, whereas its derivatives demonstrate a universal scaling at the second-order phase transitions.[5] In this section, we show how to use $\mathcal{K}_T$ to plot the low-temperature phase diagram; the analytic expression of $\mathcal{K}_T$ in strong coupling regime and its application in fixing the local minimum of Tan's contact and separating the Tomonaga–Luttinger liquid phase from the quantum critical region; and finally the scaling behavior of $\mathcal{K}_T$.

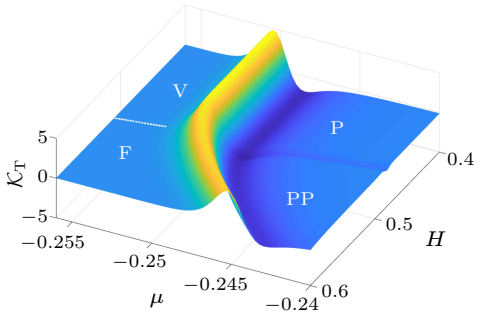


Fig. 1. Phase diagram of the attractive Gaudin–Yang model on μ–H plane by plotting the contact capacity $\mathcal{K}_T$ at $T=0.001$ and $c=-1$. V, F, P and PP respectively denote the vacuum, fully polarized phase, paired phase, and partially polarized phase, respectively.

Phase diagram Shown in Fig. 1 is the plot of $\mathcal{K}_T$ on μ–H plane with given temperature $T=0.001$ and interaction $c=-1$ by numerically solving the TBA equations[5] with a

truncation up to $n = 3$. We denote the four phases as follows: vacuum by V, fully polarized phase by F, paired phase by P, and partially polarized phase by PP. It should be noted that there is no finite temperature phase transition here, and all these phases indicate the situation in the ground state. It is obvious to see the striking enhancement of $\mathcal{K}_{\rm T}$ along the phase boundary between V & F phases and P & PP phases. This is because there is no interacting particles in either V or F, and meanwhile up- and down-spin particles coexist in both P and PP. The absence and presence of contact interaction naturally depict this phase boundary. In contrast, the phase transition between P and PP is induced by the magnetic field affording enough energy to break the bound pairs formed by up- and down-spin particles, while the contact interaction survives in both sides. Here it is reasonable that $\mathcal{K}_{\rm T}$ is not influenced so much. Between V and F, we draw a dashed line since $\mathcal{K}_{\rm T}$ can not depict the difference between the situations of no particles and of no interacting particles.

Analytical expression As is aforementioned, all the thermodynamic properties of an integrable system can be accessed through solving Eqs. (5) and (6).[15] Nevertheless, it is extremely hard to theoretically obtain the equation of state (EoS) for an arbitrarily given set of parameters. To extract the profound physics in low temperature especially close to the critical point, a closed form for EoS in strong coupling regime bridges the gap.[5–7,10,11] We hereby use this EoS to calculate the thermal-contact capacity up to $O(T/c^2)$,

$$\begin{aligned}\mathcal{K}_{\rm T} \approx & \frac{|c|}{\sqrt{2\pi T}} F^b_{\frac{1}{2}} + \frac{1}{\sqrt{2}\pi}\left(\sqrt{2}G^b_{\frac{1}{2}} + G^u_{\frac{1}{2}}\right)F^b_{\frac{1}{2}} \\ & + \frac{1}{2\pi} G^b_{-\frac{1}{2}}\left(F^b_{\frac{3}{2}} + 2\sqrt{2}F^u_{\frac{3}{2}}\right) + \frac{1}{\sqrt{2}\pi} G^b_{\frac{1}{2}} F^u_{\frac{1}{2}} \\ & + \frac{\sqrt{T}}{|c|\pi^{3/2}}\left[\frac{3}{2}G^b_{\frac{1}{2}}(\sqrt{2}G^b_{\frac{1}{2}} + 5G^u_{\frac{1}{2}})F^b_{\frac{1}{2}}\right. \\ & + G^b_{-\frac{1}{2}}\left(3G^b_{\frac{1}{2}} + \sqrt{2}G^u_{\frac{1}{2}}\right)F^u_{\frac{3}{2}} + G^b_{\frac{1}{2}} G^u_{-\frac{1}{2}} F^b_{\frac{3}{2}} \\ & \left. + \frac{5}{2}\left(G^b_{\frac{1}{2}}\right)^2 F^u_{\frac{1}{2}}\right] + \frac{\sqrt{T}}{|c|\pi^{3/2}}\left(3G^b_{\frac{1}{2}} + 5\sqrt{2}G^u_{\frac{1}{2}}\right) \\ & \times \left[\frac{1}{4\sqrt{2}}\left(G^b_{\frac{1}{2}}\right)^2 - \frac{3}{4\sqrt{2}} G^b_{\frac{1}{2}} G^b_{-\frac{1}{2}}\right] + O(T/c^2), \end{aligned} \tag{10}$$

where

$$G^d_m \equiv {\rm Li}_m\left(-{\rm e}^{\frac{A_d}{T}}\right), \quad F^d_m \equiv \frac{A_d}{T} G^d_{m-1} - m G^d_m, \tag{11}$$

with index $d = b, u$ and polylog function ${\rm Li}_n(x)$. See Appendix A for A_d.

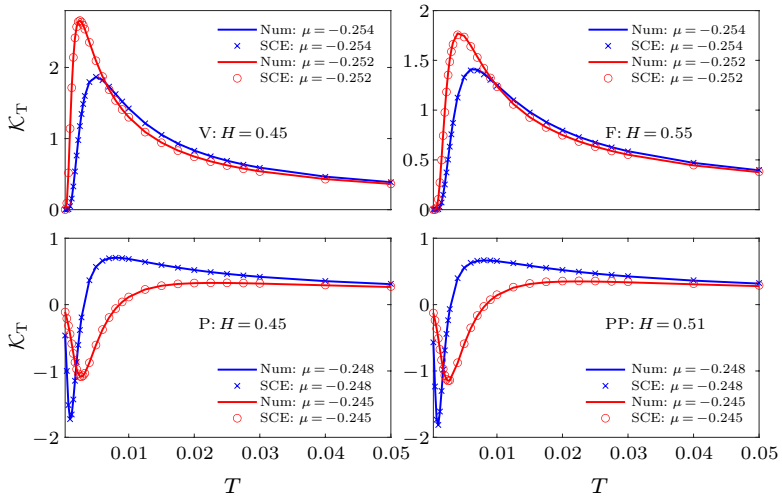


Fig. 2. The thermal-contact capacity $\mathcal{K}_{\rm T}$ vs. temperature T in different phases with given magnetic field and chemical potentials. The solid curves and symbols represent the results from numerics (NUM) and strong coupling expansion (SCE), respectively. Due to the spin-dependent interaction, there is an abrupt change for the $\mathcal{K}_{\rm T}$ and thus $\mathcal{C}$ is non-monotonic at low temperatures in phases P and PP.

Utilizing the strong coupling expansion, in Fig. 2 we study the behavior of $\mathcal{K}_{\rm T}$ versus T in four different phases in low temperatures, where the red and blue stand for curves of different chemical potentials, while the symbols and solid curves come from theoretical expression (10) and numerics respectively. The excellent agreement between the theoretical and numerical results evidences the validity of expansion up to the first few orders. It is seen clearly that in phases P and PP, $\mathcal{K}_{\rm T}$ evolves from negative to positive value indicating a local minimum of Tan's contact at a specified temperature $T_{\rm CRO}$; while in phases V and F, always $\mathcal{K}_{\rm T} > 0$. Specifically to this model of strong interaction, the contact, of much dependence on the bound states formed by pairs of particles with opposite spin directions, is approximately proportional to the number of down-spin fermions M.[5] Meanwhile, along with increase of temperature, the total charge number N and imbalance between spins $P = N_\uparrow - N_\downarrow$ change, and satisfy $\Delta M = (\Delta N - \Delta P)/2$. This implies that the change of contact reflects the competition between the changes of charge and spin degrees of freedom. Away from zero temperature, at first the increase on charge degree of freedom is less than that on spin, while it gradually and eventually overwhelms the spin

degree of freedom, where this competition is signaled by $T_{\rm CRO}$. In general, the coexistence of up- and down-spin particles determines the presence of this phenomenon, and thus it is observed uniquely in 1D multi-component systems, such as the repulsive Gaudin–Yang model[17,18] and the spinor bosons.[19] At low temperatures, the drastic change of Tan's contact takes place in a very tiny temperature interval and above this interval the contact monotonically increases with temperature. This is a reflection of the crossover from Tomonaga–Luttinger liquid (TLL) to the spin-incoherent liquid,[20] which was firstly identified in a spin-balanced system through finding the totally different shapes of momentum distribution in these two regions.[21,22] The behaviors of $\mathcal{K}_{\rm T}$ in spin-balanced and spin-imbalanced phases are similar, manifesting the key role of spin-dependent contact interaction in the crossover.

In Fig. 3 we display the $\mathcal{K}_{\rm T}$ on μ–T plane, and the three phases of finite temperature are respectively CG the classical gases, TLL$_{\rm P}$ the TLL in P phase, and QC the quantum criticality. Similar to other second derivatives of thermodynamic potential, such as the specific heat, here we use the extremum of $\mathcal{K}_{\rm T}$ represented by dashed curves to separate the above different phases.

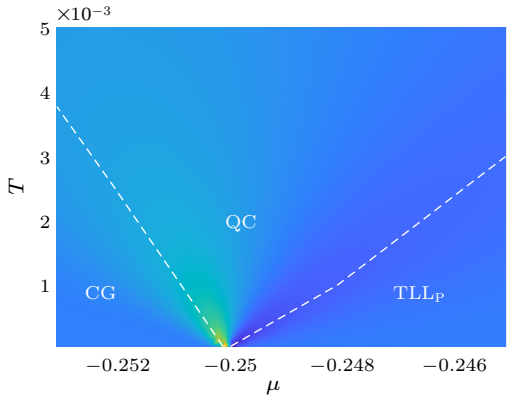


Fig. 3. A contour plot of $\mathcal{K}_{\rm T}$ on μ–T plane. Here TLL$_{\rm P}$ means the TLL in the paired phase, QC the quantum criticality and CG the classical gases. The left and right dashed curves mean the extremum of $\mathcal{K}_{\rm T}$ in phases V and P, respectively. The extremum of $\mathcal{K}_{\rm T}$ separates the low temperature phase with the quantum criticality.

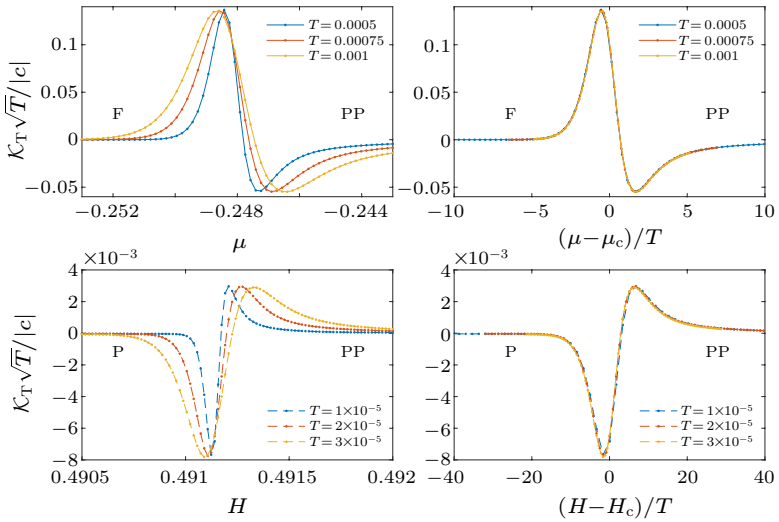


Fig. 4. The scaling behavior of thermal-contact capacity in the neighborhood of quantum critical point. The upper panel represents $\mathcal{K}\sqrt{T}/|c|$ close to the quantum critical region between the fully polarized phase and the partially polarized phase, while the lower between the paired phase and partially polarized phase. The driving parameters are the chemical potential μ and the magnetic field H, respectively. The magnetic field in the upper panel and chemical potential in the lower panel are $H = 0.55$ and $\mu = -0.245$, respectively. In the left panel, it is seen clearly that the curves of different temperatures intersect at a specified point, which is exactly the critical parameter; while the right panels shows that all these curves uniquely collapse onto the scaling relation once the argument is chosen as $(x - x_{\rm c})/T$.

Scaling laws The renormalization group theory depicts that at low temperatures, there is a universal scaling law for the thermodynamic quantities in the critical region,[23] i.e., all the second order thermodynamic quantities obey

$$\mathcal{O} = \mathcal{O}_0 + \lambda_{\mathcal{O}}\, T^{\frac{d}{z}+1-\frac{2}{\nu z}}\, \mathcal{F}\Big(\frac{\mu-\mu_{\rm c}}{T^{1/\nu z}}\Big), \tag{12}$$

where $\mathcal{O}_0$ is the background, $\lambda_{\mathcal{O}}$ the prefactor, d the dimension, z the correlation length exponent, ν the dynamical critical exponent, and $\mathcal{F}(x)$ the scaling function. Here on top of the analytical results obtained in the condition of strong coupling and low temperature in Eq. (10), we derive the scaling behavior of $\mathcal{K}_{\rm T}$ around the corresponding critical point

$$\mathcal{K}_{\rm T}^{\rm V-P} = \frac{|c|}{\sqrt{2\pi T}}\Big[2\xi \mathrm{Li}_{-\frac{1}{2}}(-\mathrm{e}^{2\xi}) - \frac{1}{2}\mathrm{Li}_{\frac{1}{2}}(-\mathrm{e}^{2\xi})\Big], \tag{13}$$

$$\mathcal{K}_{\rm T}^{\rm F-PP} = \Big(1 - \frac{1}{\pi}a^{\frac{1}{2}} + \frac{1}{\pi}a^{\frac{3}{2}}\Big)\mathcal{K}_{\rm T}^{\rm V-P}, \tag{14}$$

$$\mathcal{K}_{\rm T}^{\rm P-PP} = -\frac{|c|\sqrt{2bq}}{\pi^{3/2}\sqrt{T}}\Big[\xi \mathrm{Li}_{-\frac{1}{2}}(-\mathrm{e}^{\xi}) - \frac{1}{2}\mathrm{Li}_{\frac{1}{2}}(-\mathrm{e}^{\xi})\Big], \tag{15}$$

with prefactors

$$a = (h-1)\Big(1 + \frac{2}{3\pi}\sqrt{h-1}\Big),$$

$$b = (1-h)\Big(1 + \frac{2}{\pi}\sqrt{1-h}\Big),$$

$$q = 1 - \frac{5\sqrt{b}}{\pi} + \frac{9b}{\pi^2} - \frac{2b}{3\pi}, \tag{16}$$

where $\xi = (\mu - \mu_c)/T$, $h = H/\varepsilon_B$, and μ_c is the critical point at zero temperature. It is readily to read off the exponents $z = 2$, $\nu = 1/2$ and the scaling function responsible for the singular behavior $\mathcal{F}(x) = \mathrm{Li}_{-\frac{1}{2}}(-\mathrm{e}^x)$. Note that $\mathrm{Li}_{-\frac{1}{2}}(x)$ is the aforementioned Polylog function. It is interesting to see that the scaling behavior of $\mathcal{K}_T$ between V and P is almost the same as that between F and PP, due to the same mechanism that the system of no interaction evolves into an interacting status. This is in accordance with the phase diagram shown in Fig. 1, where the drastic enhancement of $\mathcal{K}_T$ occurs along the specified phase boundary between V and F as well as between P and PP.

Utilizing the scaling relation of Eq. (12), a scheme to map out the critical point from the finite temperature data was proposed.[24] Here we numerically solve the TBA equations, and thus in Fig. 4 we arrive at the thermal-contact capacity of different temperatures. In the left panel, the intersection of those curves determine the critical parameters, and thus we have the critical chemical potential $\mu_c = -0.2482$ and the critical magnetic field $H_c = 0.4911$; while the right panel shows that the curves collapse into the scaling function by setting the proper argument $(x - x_c)/T$. Moreover, the amplitudes of scaling relations across different phase boundaries are disparate so that the one between F and PP is much larger than that between P and PP. This can also be seen clearly in Fig. 1.

4. Conclusion

A through study on the thermal-contact capacity $\mathcal{K}_T$ in the attractive Gaudin–Yang model has been presented by numerically and analytically solving the TBA equations. It is shown that $\mathcal{K}_T$ is useful in identifying the low temperature phase diagram where the significant enhancement of $\mathcal{K}_T$ clearly marks the phase boundary between phases V and P as well as phases F and PP, manifesting the role of interaction in this process. By virtue of the strong coupling expansion, we derive an analytical expression of $\mathcal{K}_T$, and the involved generating functions give an access to its critical behavior and the scaling law. Following this, both the critical exponents and scaling function are readily obtained, and the curves of $\mathcal{K}_T$ at different temperatures in different quantum critical regions map out the correct critical points. It should be noted that in a tiny temperature interval, $\mathcal{K}_T$ indicates the contact $\mathcal{C}$ is non-monotonic along with the temperature, and above this interval, however, always increase gradually. This phenomenon is observed in either spin-balanced or imbalanced phases, implying the crossover from the TLL to spin-coherent liquid. A reconstruction of the momentum distribution can be observed. This research will deepen our understanding on the performance of contact near the critical point and its relation with other driving parameters in a dilute system.

Appendix A

$$T_{mn}(\lambda) = \begin{cases} a_{|n-m|}(\lambda) + 2a_{|n-m|+2}(\lambda) + \cdots + 2a_{m+n-2}(\lambda) \\ \quad + a_{m+n}(\lambda), \quad \text{for } m \neq n, \\ 2a_2(\lambda) + 2a_4(\lambda) + \cdots + 2a_{2n-2}(\lambda) + a_{2n}(\lambda), \\ \qquad\qquad \text{for } m = n. \end{cases}$$

$$A_b \approx 2\mu + \frac{c^2}{2} + \frac{T^{\frac{3}{2}}}{\sqrt{2\pi}|c|} G^b_{\frac{3}{2}} + \frac{2T^{\frac{3}{2}}}{\sqrt{\pi}|c|} G^u_{\frac{3}{2}},$$

$$A_u \approx \mu + \frac{H}{2} + \frac{\sqrt{2}T^{\frac{3}{2}}}{\sqrt{\pi}|c|} G^b_{\frac{3}{2}}.$$

Acknowledgments

Project supported by the National Natural Science Foundation of China (Grant Nos. 12104372, 12047511, and 12247103) and the Youth Innovation Team of Shaanxi Universities.

References

[1] Tan S 2008 *Ann. Phys.* **323** 2952
[2] Tan S 2008 *Ann. Phys.* **323** 2971
[3] Tan S 2008 *Ann. Phys.* **323** 2987
[4] Barth M and Zwerger W 2011 *Ann. Phys.* **326** 2544
[5] Chen Y Y, Jiang Y Y, Guan X W and Zhou Q 2014 *Nat. Commun.* **5** 5140
[6] He W B, Chen Y Y, Zhang S Z and Guan X W 2016 *Phys. Rev. A* **94** 031604(R)
[7] Peng L, Yu Y C and Guan X W 2019 *Phys. Rev. B* **100** 245435
[8] Yang C N 1967 *Phys. Rev. Lett.* **19** 1312
[9] Gaudin M 1967 *Phys. Lett. A* **24** 55
[10] Guan X W, Yin X G, Foerster A, Batchelor M T, Lee C H and Lin H Q 2013 *Phys. Rev. Lett.* **111** 130401
[11] Guan X W and Ho T L 2011 *Phys. Rev. A* **84** 023616
[12] Lee J Y and Guan X W 2011 *Nucl. Phys. B* **853** 125
[13] Liao Y A, Rittner A S C , Paprotta T, Li W, Partridge G B, Hulet R G, Baur S K and Mueller E J 2010 *Nature* **467** 567
[14] Guan X W, Batchelor M T and Lee C H 2013 *Rev. Mod. Phys.* **85** 1633
[15] Takahashi M 1999 *Thermodynamics of One-Dimensional Solvable Models* (Cambridge: Cambridge University Press)
[16] Please refer to chapter 13 of Ref. [15] for a more detailed explanation.
[17] Capuzzi P and Vignolo P 2020 *Phys. Rev. A* **101** 013633
[18] Pâțu O I and Klümper A 2016 *Phys. Rev. A* **93** 033616
[19] Pâțu O I, Klümper A and Foerster A 2018 *Phys. Rev. Lett.* **120** 243402
[20] Fiete G A 2007 *Rev. Mod. Phys.* **79** 801
[21] Cheianov V V and Zvonarev M B 2004 *Phys. Rev. Lett.* **92** 176401
[22] Cheianov V V, Smith H and Zvonarev M B 2005 *Phys. Rev. A* **71** 033610
[23] Fisher M P A, Weichman P B, Grinstein G and Fisher D S 1989 *Phys. Rev. B* **40** 546
[24] Zhou Q and Ho T L 2010 *Phys. Rev. Lett.* **105** 245702